Journal of Sound and Vibration 325 (2009) 835–851

Contents lists available at ScienceDirect

Journal of Sound and Vibration

journal homepage: www.elsevier.com/locate/jsvi

Sound radiation characteristics of a box-type structure ☆

Tian Ran Lin [a,*], Jie Pan [b]

[a] School of Engineering Systems, Queensland University of Technology, 2 George Street, Brisbane, Qld 4001, Australia
[b] School of Mechanical Engineering, University of Western Australia, 35 Stirling Highway, Crawley, WA 6009, Australia

ARTICLE INFO

Article history:
Received 17 June 2007
Received in revised form
7 April 2009
Accepted 10 April 2009
Handling Editor: L.G. Tham
Available online 14 May 2009

ABSTRACT

The finite element and boundary element methods are employed in this study to investigate the sound radiation characteristics of a box-type structure. It has been shown [T.R. Lin, J. Pan, Vibration characteristics of a box-type structure, *Journal of Vibration and Acoustics, Transactions of ASME* 131 (2009) 031004-1–031004-9] that modes of natural vibration of a box-type structure can be classified into six groups according to the symmetry properties of the three panel pairs forming the box. In this paper, we demonstrate that such properties also reveal information about sound radiation effectiveness of each group of modes. The changes of radiation efficiencies and directivity patterns with the wavenumber ratio (the ratio between the acoustic and the plate bending wavenumbers) are examined for typical modes from each group. Similar characteristics of modal radiation efficiencies between a box structure and a corresponding simply supported panel are observed. The change of sound radiation patterns as a function of the wavenumber ratio is also illustrated. It is found that the sound radiation directivity of each box mode can be correlated to that of elementary sound sources (monopole, dipole, etc.) at frequencies well below the critical frequency of the plates of the box. The sound radiation pattern on the box surface also closely related to the vibration amplitude distribution of the box structure at frequencies above the critical frequency. In the medium frequency range, the radiated sound field is dominated by the edge vibration pattern of the box. The radiation efficiency of all box modes reaches a peak at frequencies above the critical frequency, and gradually approaches unity at higher frequencies.

1. Introduction

Sound radiation from vibrating structures has long been an interesting research topic. Many previous and recent researches focused on sound radiation [1] of simple structural components such as flat plate panels [2], ribbed panels [3] or cylindrical shells [4,5] because they are the few radiation problems that can be solved analytically. Efforts have also been made towards the numerical solution for sound radiation of three-dimensional structures of arbitrary shapes [6,7]. However, little has been reported on sound radiation characteristics of box-type structures even though this type of structures has broad engineering applications. Box-type structures are typical structures used for machine covers, transformation tanks, etc., which usually consist of plate panels connected at their common edges and include more details

☆ Some of the results were presented in "Sound radiation from a box-type structure", Proceedings of Inter-Noise 2001, The Hague, The Netherlands, August 2001, pp. 803–808.

* Corresponding author. Tel.: +61 7 3138 1272; fax: +61 7 3138 8381.
E-mail address: trlin@qut.edu.au (T. Ran Lin).

0022-460X/$ - see front matter © 2009 Elsevier Ltd. All rights reserved.
doi:10.1016/j.jsv.2009.04.016

like cut-outs and stiffening members. They are excited dynamically, vibrate and radiate sound to cause noise problems. This study aims to disclose the common features of modal vibration and sound radiation of box type structures so that effective control approaches can be implemented to address the noise problem of such structures.

Computational techniques have been employed in the last few decades to solve the vibro-acoustic problems of complex structures due to the rapid advanced of computer technologies and the increasing complexity of analytical work for complex problems. Boundary element method (BEM) has been proved to be an accurate approach to exterior acoustic problems, and is increasingly used for examining sound radiation characteristics of complex structures [8]. Boundary element methods in acoustics are based on numerical solution of the Helmholtz integral equation on the boundary of the geometry domain of a structure. Comparing to other numerical solutions, such as finite element analysis or finite difference method, BEM has great advantage in solving exterior sound radiation problems. By invoking the Sommerfeld radiation condition, only the finite boundary of a radiation structure needs to be discretized. Thus, much less computational effort is required. For instance, Seybert et al. [9] employed computational and experimental techniques to assess the accuracy of using finite element and boundary element analysis for predicting sound radiation from a box structure. In their work, only one panel of the box is flexible, the other panels are effectively rigid in the frequency range of their investigation. Most recently, Lin and Pan [1] showed that modes of natural vibration of a box-type structure (consisting of six flexural panels) can be classified into six groups according to the symmetry properties of the three panel pairs forming the box. Elementally sound sources such as monopole, dipole etc. were identified in the box modes having large global or local volume displacements.

In this paper, characteristics of sound radiation of a box-type structure in relation to the symmetrical properties in box vibration [1] are investigated. The study aims to illustrate the general physical features of sound radiation of a box-type structure rather than to develop a new analytical technique, in the hope that such understanding can lead to the noise control of practical engineering applications such as noise radiation from the cover of an air conditioner or from a transformer tank. Hence, existing BEM tool (i.e., the "Direct collocation BEM method") based on SYSNOISE [10] is utilized in the study. The non-uniqueness problem in the direct collocation BEM [8] is overcome by the so-called CHIEF approach by applying over-determined nodal points inside the enclosed cavity and assigning zero pressure to those points. Details of the theoretical and computational basis of this method can be found in Refs. [8,10].

Results of modal sound radiation of only one box-type structure are used in this study although vibration and sound radiation of other box structures have also been calculated. It is found [1] that the classification of mode shapes according to the symmetrical properties of a box structure is the same regardless of the box dimension. The mode shape and modal frequency of a box mode will adapt to the changing box dimension since it is governed by the wave matching conditions between the plate bending wave and the panel dimensions of the box. Modal sound radiation of box structures of other dimensions will closely adapt to the change of box modal vibration, but it is still governed by the same principles outlined in this work and in Ref. [1]. Increasing complexity of vibration and sound radiation analysis arising from a practical structure with reduced symmetry can also be investigated by studying the effect of asymmetry of the structure on the vibration and sound radiation of a box-type structure using similar approaches employed in this work and in Ref. [1].

The study of modal vibration and sound radiation of a box type structure also provides useful information for the prediction of noise and vibration response of such structures under external excitations. For instance, when a box structure is excited by a broadband noise inside the box or is driven by broadband forces at one or more panels, the vibration response of the box is the sum of resonance response of the box modes. The sound field external to the box is dominated by sound radiation of high radiation efficient modes (i.e., the large volume displacement modes). Therefore, the vibration response and noise radiation of a box structure driven by external sources can be predicted once the modal vibration and sound radiation characteristics of the box are known. Control of noise radiation from a box structure, e.g., the machine cover of an air conditioner, thus can be simplified to the control of modal vibration of a few large volume displacement modes (whose modal sound radiation dominates the sound field).

Accuracy of the direct BEM method based on SYSNOISE is examined in the study for three simple cases where analytical solutions are available: (1) radiation efficiencies for a number of simply supported panel modes (the (1,1), (1,2), (2,2), (1,6) and (1,7) modes) predicted by direct BEM approach were compared to those given by Wallace [2]. Good agreements were found for all corresponding radiation efficiency curves at low, medium and high wavenumber ratios; (2) the radiation efficiency of a vibrating spherical surface (radius $a = 0.1$ m) predicted by direct BEM was compared to the analytical solution given by Norton [11], the error is <0.02 percent for ka up to 2.7 where k is the acoustic wavenumber in air; and (3) sound pressures at positions between 0.1 and 10 m (in 0.1 m increment) away from the vibrating spherical surface in Case B predicted by BEM were compared with those predicted by the analytical solution at one single frequency. The error range was found <1.3 percent. Furthermore, the indirect variational method in SYSNOISE was also used to calculate the radiation efficiency of a few box modes at a number of random chosen frequencies, the results agree quite well to those obtained by direct collocation BEM method at those frequencies.

Section 2 presents a detail description of the box structure used in this study and provides a brief summary of its modal vibration characteristics. The common features of modal radiation efficiencies for the six groups of box modes [1] are studied in Section 3. Patterns of modal sound radiation directivity from each group of modes are examined in Section 4 at frequencies ranging from far below to well above the critical frequency. Conclusions are given in Section 5.

2. Description of the box structure and its modal characteristics

The box structure used in this study is the same as that used in Ref. [1]. It is a rectangular parallelepiped box consisting of three pairs of rectangular panels as shown in Fig. 1. The dimensions of the box are chosen to be the same as the panel-cavity system used in Ref. [12], where general conclusions of the interaction between internal sound field and a box structure were drawn. All plate panels have the same thickness of 2.5 mm, and are made of aluminum of Young's modulus $E = 7.1 \times 10^{10}\,\mathrm{N/m^2}$, density $\rho = 2700\,\mathrm{kg/m^3}$ and Poisson's ratio $\nu = 0.3$. The edges of the box are free in six degrees of freedom. A spherical coordinate system with origin at the center of the box $(L_x/2, L_y/2, L_z/2)$, as shown in Fig. 1, is used to describe the radiated sound pressure at (r,θ,φ).

Vibration characteristics of the box structure are studied and discussed in detail in Ref. [1]. A brief summary is given here as an introduction to the study of sound radiation characteristics of the box structure. The natural vibration modes of a box structure can be classified into six groups according to the symmetrical properties of the three panel pairs constituting the box [1]. Vibration distribution in a pair of panels is symmetrical if corresponding points in the two parallel panels move simultaneously inwards or outwards with respect to the un-deformed box. It is asymmetrical if each two corresponding points move one inwards and the other outwards at the same instant. The mode shape distribution in the box panels and the natural frequencies were found to be governed by the wave matching condition between the plate bending wave and the physical dimension of the panels [1]. The panel pair whose dimensions best matching the plate bending wavelength at the modal frequency has the maximum amplitude distribution, and is termed the dominant panel pair. The other two panel pairs are non-dominant.

According to the symmetrical properties and vibration distribution of the three panel pairs constituting the box, the modes are classified into six groups: (1) Group (D_S, S, S), where the dominant panel pair and the two non-dominant panel pairs are all symmetrical; (2) Group (D_S, S, AS), where the dominant panel pair and one non-dominant pair are symmetrical, the other non-dominant pair is asymmetrical; (3) Group (D_S, AS, AS), where the dominant pair is symmetrical and the other two pairs are asymmetrical; (4) Group (D_AS, AS, AS), where all three panel pairs are asymmetrical; (5) Group (D_AS, AS, S), where the dominant panel pair and one non-dominant pair are asymmetrical, the other non-dominant pair is symmetrical; and (6) Group (D_AS, S, S), where the dominant panel pair is asymmetrical and the other two pairs are symmetrical.

According to this classification, the box mode depicted in Fig. 2 can be described by $[D\_AS(2,1), AS(2,1), S(2,2)^*]_{30.8\,\mathrm{Hz}}$. In this description, the three elements in the bracket describe the modal vibration distribution of the three panel pairs of the box. The first element indicates that the panel pair perpendicular to the x axis of the global coordinate system is a dominant asymmetrical panel pair whose mode shape distribution is described by the (2, 1) mode of a simply supported panel. The first index in the parenthesis is the number of anti-nodes in the y-direction and the second index is the number of anti-nodes in z-direction for the panel pair. The second element indicates that the panel pair perpendicular to the y-axis also has the (2, 1) mode shape and vibrates asymmetrically. Symmetrical vibration is identified in the third panel pair (the pair perpendicular to the z-axis) whose mode shape is described by the third element $S(2,2)^*$. The asterisk following the indices indicates that the amplitude distribution of this panel pair is somewhat distorted from the (2, 2) mode of a simply supported panel. Finally, the frequency (30.8 Hz) following the bracket represents the natural frequency of the mode. Table 1 lists the first 33 non-rigid body modes of the box structure and the associated net volume displacements [1].

The classification of free vibration modes of the box has assisted the understanding of vibration characteristics of a box-type structure in terms of total and local volume displacements, and contributions from in-plane and out-of-plane vibration [1]. In this paper, it is shown that the symmetrical properties of the box vibration also correlate to modal sound

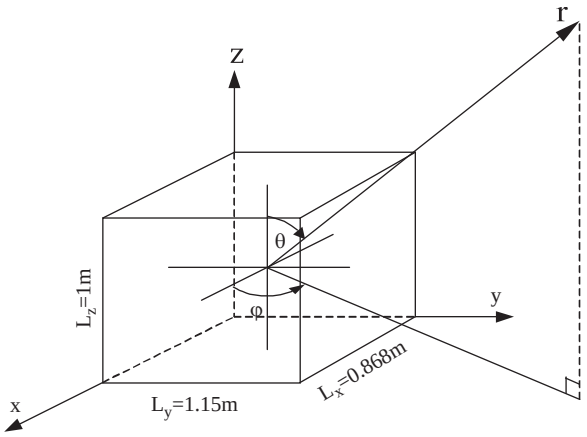

Fig. 1. Coordinate systems of the box-type structure.

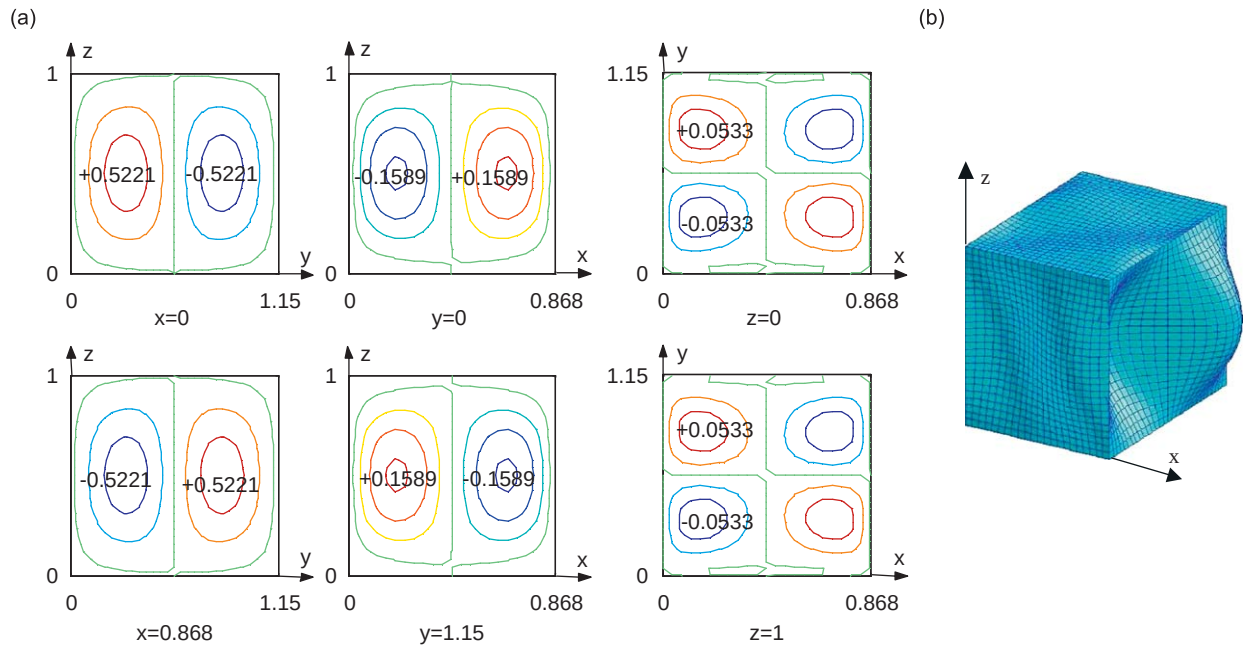

Fig. 2. Amplitude distribution of mode $[D\_AS(2,1), AS(2,1), S(2,2)^*]_{30.8\,\mathrm{Hz}}$: (a) contour plots and (b) isometric view.

Table 1
Classification of the first 33 modes and associated net-volume displacements.

Group	Mode shape description	Net-volume displacement $\sum_{n=1}^{6}(\sum_m \Delta V_m)_n$
(D_S, S, S)	$[D\_S(1,1), S(1,1)^*, S(1,1)]_{13.5\,\mathrm{Hz}}$	0.1180
	$[S(1,1)^*, S(1,1), D\_S(1,1)]_{18.0\,\mathrm{Hz}}$	0.1194
	$[S(1,1), D\_S(1,1), S(1,1)]_{23.0\,\mathrm{Hz}}$	0.6355
	$[D\_S(3,1), S(1,3)^*, S(1,3)]_{54.1\,\mathrm{Hz}}$	0.0633
	$[S(3,1), S(1,1)^*, D\_S(1,3)]_{57.3\,\mathrm{Hz}}$	0.1839
	$[D\_S(1,3), S(1,3)^*, S(3,1)]_{66.6\,\mathrm{Hz}}$	0.0975
(D_S, S, AS)	$[D\_S(2,1), AS(1,1)^*, S(1,2)]_{30.3\,\mathrm{Hz}}$	0
	$[S(2,1), AS(1,1), D\_S(1,2)]_{35.8\,\mathrm{Hz}}$	0[a]
	$[D\_S(1,2), S(1,2), AS(1,1)^*]_{36.4\,\mathrm{Hz}}$	0
	$[S(1,2), D\_S(1,2), AS(1,3)^*]_{40.5\,\mathrm{Hz}}$	0
	$[AS(3,1)^*, D\_S(2,1), S(2,1)]_{43.5\,\mathrm{Hz}}$	0
	$[AS(1,1)^*, S(2,1), D\_S(2,1)]_{45.7\,\mathrm{Hz}}$	0
	$[D\_S(3,2), S(3,2)^*, AS(1,3)]_{76.0\,\mathrm{Hz}}$	0
(D_S, AS, AS)	$[D\_S(2,2), AS(1,2), AS(1,2)]_{52.7\,\mathrm{Hz}}$	0[a]
	$[AS(2,3)^*, AS(2,1), DS(2,2)]_{60.3\,\mathrm{Hz}}$	0
	$[AS(3,2), D\_S(2,2), AS(2,3)^*]_{65.6\,\mathrm{Hz}}$	0
(D_AS, AS, AS)	$[D\_AS(2,2), AS(2,2)^*, AS(2,2)]_{48.9\,\mathrm{Hz}}$	0
	$[AS(2,2)^*, AS(2,2), D\_AS(2,2)]_{61.0\,\mathrm{Hz}}$	0
	$[AS(2,2)^*, D\_AS(2,2), AS(2,2)]_{71.0\,\mathrm{Hz}}$	0[a]
(D_AS, AS, S)	$[D\_AS(2,1), AS(2,1), S(2,2)^*]_{30.8\,\mathrm{Hz}}$	0
	$[S(2,2)^*, AS(1,2), D\_AS(1,2)]_{32.8\,\mathrm{Hz}}$	0
	$[D\_AS(1,2), S(2,2)^*, AS(2,1)]_{34.7\,\mathrm{Hz}}$	0
	$[S(2,2), D\_AS(1,2), AS(1,2)^*]_{42.0\,\mathrm{Hz}}$	0
	$[AS(4,1)^*, D\_AS(2,1), S(2,2)]_{49.2\,\mathrm{Hz}}$	0
	$[AS(1,2)^*, S(2,2), D\_AS(2,1)]_{50.2\,\mathrm{Hz}}$	0
	$[D\_AS(3,2), S(2,2), AS(2,3)]_{76.6\,\mathrm{Hz}}$	0
(D_AS, S, S)	$[D\_AS(1,1), S(2,1), S(2,1)]_{17.2\,\mathrm{Hz}}$	0
	$[S(1,2), S(1,2), D\_AS(1,1)]_{19.5\,\mathrm{Hz}}$	0
	$[S(2,1), D\_AS(1,1), S(1,2)]_{20.9\,\mathrm{Hz}}$	0
	$[S(3,2), S(1,2)^*, D\_AS(1,3)]_{60.7\,\mathrm{Hz}}$	0
	$[D\_AS(3,1)*, S(2,1), S(2,3)]_{61.7\,\mathrm{Hz}}$	0
	$[S(2,3)^*, D\_AS(1,3), S(1,4)]_{72.3\,\mathrm{Hz}}$	0
	$[D\_AS(1,3), S(2,3)^*, S(2,1)]_{74.9\,\mathrm{Hz}}$	0

Note: Panels $n = 1, 2, 3, 4, 5$ and 6 are those at $x = 0$, L_x, $y = 0$, L_y, and $z = 0$, L_z, respectively.
ΔV_m is the volume displacement associated with the normal amplitude displacement of the mth element in a panel.
[a] Indicates the mode that generates a large volume displacement locally although the net volume displacement is nil.

radiation characteristics of the six mode groups. Modal radiation characteristics of the box structure are studied in this paper by the following two features:

(1) Modal radiation efficiency σ as a function of the wavenumber ratio $\gamma = k/k_p$ for modes in the six groups, where k_p is the modal wavenumber of the dominant plate panels which is calculated by using the modal indices of the corresponding simply supported panel given in the mode shape description. The radiation efficiency is calculated from [10]

$$\sigma = \frac{W_{\text{rad}}}{W_{\text{in}}}, \tag{1}$$

where W_{rad} is the radiated sound power, which is obtained by integrating the active normal intensity over the radiating surface, W_{in} is the sound power radiated by a large rigid piston with the same surface area of the structure and vibrating with the same root mean squared velocity [11]. It is calculated by integrating the square of the normal velocity over the surface of the box structure using the modal vector of the structure. The radiation efficiency σ in Eq. (1) is actually a ratio, which can take values greater than unity. While it is called "radiation ratio" in some references [11], some more recent publications [8,13] still use the name "radiation efficiency".

(2) Sound radiation pattern for each box mode is evaluated on a spherical surface of the radius $r = 10$ m from the center of the box. Modal radiation patterns at frequencies below and above the critical frequency are presented in this study to illustrate the successively change of directivity patterns.

3. Modal radiation efficiency

The radiation efficiency of the box modes in the low, medium and high frequency ranges is studied in this section. Slopes of modal radiation efficiency curves for the six groups of modes are compared to those of the corresponding simply supported panel modes in the low frequency range. Plateau or change in slope in the radiation efficiency curve of higher order box modes in the medium frequency range is examined. Effects of local volume displacement, mode shape, phase distribution of the dominant panel pair and the relative phase between the adjacent panels on the radiation efficiency of the box modes are also discussed.

3.1. Characteristics of modal radiation efficiencies of the six mode groups

Fig. 3a–f shows the radiation efficiency σ as a function of the wavenumber ratio γ for typical modes of the six groups. Modes from each group are selected in this simulation such that they cover a range of radiation efficiency from the highest to the smallest values at low frequencies in their respective group in the frequency range of investigation. Natural frequencies of modes used in this study cover the frequency range up to 109.7 Hz [14]. Values of wavenumber ratios, corresponding to the modal natural frequencies, vary from $\gamma = 0.059$ for the lowest mode at 13.5 Hz to $\gamma = 0.159$ for the highest mode at 109.7 Hz. It is shown that the radiation efficiency of all box modes has the similar trend ($\sigma \geqslant 1$) at frequencies above the critical frequency ($\gamma > 1$). Mode $[S(1,1), D\_S(1,1), S(1,1)]_{23.0\,\text{Hz}}$ from the first group (a monopole source) has the highest radiation efficiency for $\gamma < 1$ (see Fig. 3(a)) due to the large net-volume displacement generated by the modal vibration of the box mode. High modal radiation efficiency is also the case for the (1, 1) mode of a simply supported panel [2]. Modes in the first group generally have higher radiation efficiency than modes in the other groups at low γ due to the globally net-volume displacement generated by modes in this group resulting from the (odd, odd) mode shape distribution in all three panel pairs.

Modes having large local volume displacements also have the highest radiation efficiency in their respective groups for $\gamma < 1$. For example, mode $[S(2,1), AS(1,1), D\_S(1,2)]_{35.8\,\text{Hz}}$ whose modal vibration generates a large local volume displacement on each half of the box has the highest efficiency in its own group for $\gamma < 1$ (see Fig. 3(b)). So are mode $[D\_S(2,2), AS(1,2), AS(1,2)]_{52.7\,\text{Hz}}$ (a quadrupole source, Fig. 3(c)), and mode $[AS(2,2)^*, D\_AS(2,2), AS(2,2)]_{71.0\,\text{Hz}}$ (an octopole source, Fig. 3(d)). It is observed that higher order modes usually have higher radiation efficiency σ than that of lower order modes in the same group for $\gamma < 1$ except for modes that generate large global or local volume displacements. This observation is consistent to that found for modal radiation of simply supported panels [2] with the exception of the group of net-volume displacement modes.

For (odd, odd) modes in a panel, lower order modes (e.g., the (1, 1) mode) always have higher net volume displacement and therefore, higher radiation efficiency than that of higher order modes for $\gamma < 1$ [2]. In contrast, higher order net volume displacement modes of the box can have higher radiation efficiency than that of the lower order modes for $\gamma < 1$ as indicated in Fig. 3(a). Such interesting sound radiation feature is attributed to the effect of relative phase between the different panel pairs on the modal sound radiation. For example, vibrations of all three panel pairs for mode $[S(1,1), D\_S(1,1), S(1,1)]_{23.0\,\text{Hz}}$ are in phase (i.e., adjacent panels move together inwards or outwards with respect to the undeformed box), which produces a strong net volume displacement sound source (a monopole source) to give higher radiation efficiencies. Mode $[S(1,3), S(3,1), D\_S(3,1)]_{97.0\,\text{Hz}}$ is also an efficient sound radiator due to the same reason, which

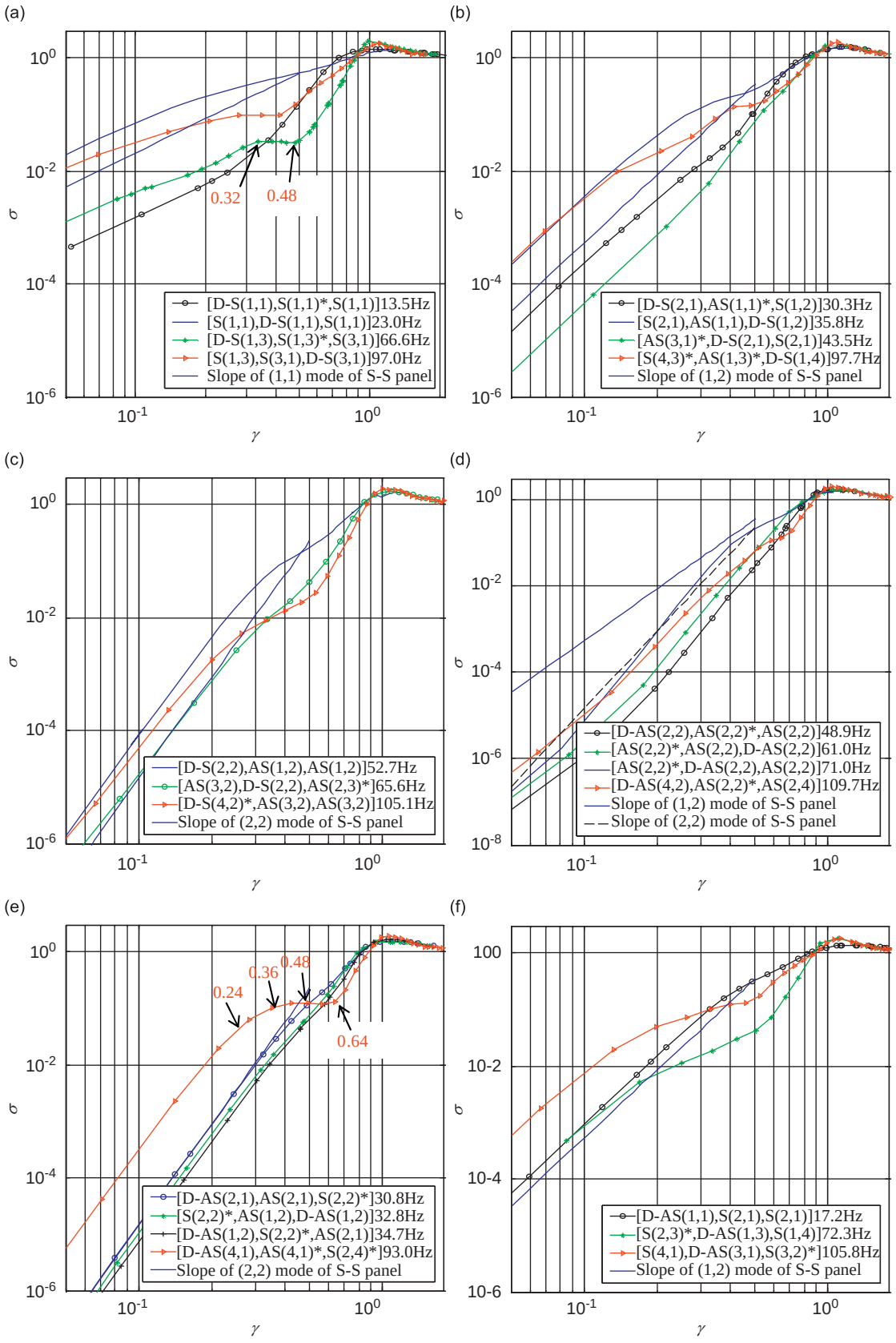

Fig. 3. Radiation efficiencies of the typical modes from the six groups: (a) (D_S, S, S); (b) (D_S, S, AS); (c) (D_S, AS, AS); (d) (D_AS, AS, AS); (e) (D_AS, AS, S); and (f) (D_AS, S, S). *Node*: In each figure, the slope of the simply supported panel modes is only valid for low value of γ.

generates comparatively large net-volume displacement [14] even though it has higher order mode shape distribution for all its panels. In contrast, the two non-dominant panel pairs of mode $[D\_S(1,1), S(1,1)^*, S(1,1)]_{13.5\,\mathrm{Hz}}$ vibrate out of phase to the dominant panel pair leading to a weaker modal sound radiation. (Note that figures of the vibration distribution of the modes discussed above were presented in Ref. [1].)

3.2. Slope of radiation efficiency curves in the low frequency range

The radiation efficiency curves for each group of modes have similar slopes for low values of γ. This is because the modal vibration for each group of modes is such that the box forms approximately the same type of elementary sound sources, i.e., monopole, dipole, quadrupole and octopole in the low frequency range. The modal radiation patterns are discussed in more details in Section 4.

3.2.1. Group (D_S, S, S)

Fig. 3(a) shows that radiation efficiency curves for modes in this group have the same slope as that of the (odd, odd) mode of a simply support panel (surface area $1.15\times1\,\mathrm{m}^2$ and 2.5 mm in thickness) in the low frequency range ($\gamma\ll1$). All modes in this group have global net volume displacements and behave as monopole sound sources at low frequencies. A slope of 20 dB/decade at low frequencies can be evaluated by the following relation from the radiation efficiency of (odd, odd) modes of a simply supported panel [2]:

$$\sigma_{m,n}\approx\frac{32k^2l_xl_y}{m^2n^2\pi^5}\propto k^2,\quad kl_x,kl_y\ll1, \tag{2}$$

where l_x, l_y are the panel dimensions and m, n are the panel modal indices. The slope of radiation efficiency curve of the (1, 1) mode of the simply supported panel at low frequencies is shown by the thick solid line in Fig. 3(a).

3.2.2. Groups (D_S, S, AS) and (D_AS, S, S)

Both the (odd, even) simply supported panel modes and these two groups of box modes have dipole radiation pattern in the low frequency range. For these two groups, as shown in Fig. 3(b) and (f), the slope of modal radiation efficiency curves is the same as that of (odd, even) mode of a simply supported panel in the low frequency range. It is 40 dB/decade as can be obtained from the relation [2]

$$\sigma_{m,n}\approx\frac{8k^4l_xl_y^3}{3m^2n^2\pi^5}\propto k^4,\quad kl_x,kl_y\ll1. \tag{3}$$

The slope of radiation efficiency curve of the (1, 2) mode of the simply supported panel at low frequencies is shown in Fig. 3(b) and (f) by the thick solid line.

3.2.3. Groups (D_S, AS, AS) and (D_AS, AS, S)

Slopes of radiation efficiency curves for modes in these two groups are similar to that of (even, even) modes of simply supported panels in the low frequency range. They are all quadrupole sound radiators in this frequency range. A slope of 60 dB/decade can be evaluated from the radiation efficiency of (even, even) modes of a simply supported panel [2] as given by Eq. (4). This slope is shown in Fig. 3(c) and (e) by the thick solid line, which is evaluated for the (2, 2) mode of the simply supported panel:

$$\sigma_{m,n}\approx\frac{2k^6l_x^3l_y^3}{15m^2n^2\pi^5}\propto k^6,\quad kl_x,kl_y\ll1. \tag{4}$$

3.2.4. Group (D-AS, AS, AS)

Because of the three dimensional nature of a box-type structure, there is another type of elementary sound source in addition to the monopole, dipole and quadrupole mentioned above. It is termed "octopole" in this paper, which is a sound source that consists of two parallel quadrupoles, 180° out-of-phase to each other. Due to the complexity in the radiation pattern for this type of sound sources, there is no existing analytical solution to be used for comparison. However, sound radiation characteristics of an octopole at low γ can be explored by comparing its radiation efficiency curve to the slopes of a dipole and a quadrupole. In Fig. 3(d), radiation efficiencies of the (1, 2) and (2, 2) modes of the simply supported panel are plotted (in thick solid and dashed lines, respectively) alongside the sound radiation efficiencies of the typical modes from this group. It is observed that in the very low frequency range ($\gamma<0.1$), radiation efficiencies of modes in this group have similar slope to that of the (1, 2) mode of a simply supported panel (i.e., a dipole), which is 40 dB/decade. In the low and medium frequency range, the slope is similar to that of a quadrupole, which is 60 dB/decade. The only exception to this observation is mode $[AS(2,2)^*, D\_AS(2,2), AS(2,2)]_{71.0\,\mathrm{Hz}}$, whose slope is slightly steeper than the other modes in the same group in the medium frequency range and is proportional to k^7, or 70 dB/decade. This is due to the large volume

displacement generated locally at the eight box corners by the modal vibration (see Ref. [1, Fig. 9] for visualization of this mode shape).

3.3. The plateau in radiation efficiency curves of higher order modes in the medium frequency range

Plateau or change in slope can be clearly observed in the radiation efficiency curves of higher order modes in each group at medium frequencies, e.g., mode $[D\_S(1,3), S(1,3)^*, S(3,1)]_{66.6\,\mathrm{Hz}}$ and mode $[S(1,3), S(3,1), D\_S(3,1)]_{97.0\,\mathrm{Hz}}$ in Fig. 3(a). Simply supported panels show similar behavior, which manifests itself as waviness in the radiation efficiency curves of higher order modes [2,13]. For higher order modes of a simply supported panel, waviness in the modal radiation efficiency curve at medium frequencies is due to the interference of sound radiated by the vibrating lobes of higher order modes when the distance between nodal lines of a vibrating mode is in the same order of the acoustic wavelength. Sound radiation of higher order box modes is also subjected to such interference in the medium frequency range. In addition, the radiation efficiency of the box modes is affected by the interference of sound radiated by each panel pair and the interference of sound radiated by neighboring panels. For better understand of this mechanism, the slope change of radiation efficiency curves of two higher order modes—mode $[D\_S(1,3), S(1,3)^*, S(3,1)]_{66.6\,\mathrm{Hz}}$ (see Fig. 3(a)) and mode $[D\_AS(4,1), AS(4,1)^*, S(2,4)^*]_{93.0\,\mathrm{Hz}}$ (see Fig. 3(e)) in the medium frequency range (somewhere between $\gamma = 0.2$ and 0.7) are examined.

Although all three panel pairs of mode $[D\_S(1,3), S(1,3)^*, S(3,1)]_{66.6\,\mathrm{Hz}}$ are symmetrical, only the first and the third pairs are important to the sound radiation because the second pair has much smaller vibration amplitude (see Ref. [1, Fig. 5]). The two-dimensional cross section (parallel to the x–z plane) mode shape distribution of the first and the third panel pairs of this mode is shown in Fig. 4(a). Because of the higher order mode shape distribution of the panels and the out-of-phase distribution between adjacent cells of the neighboring panels, the net-volume displacement generated by this mode is small [1]. This leads to a less effective sound radiator for low γ.

A plateau in the radiation efficiency curve is observed in the medium γ range resulting from wave interference. The plateau begins at somewhere between $\gamma = 0.32$ and 0.37 where the increasing sound radiation efficiency of panel vibration is completely offset by the increasing wave interference between sound radiated by the component panels. At $\gamma = 0.32$ where the acoustic wavelength λ equals twice the distance of the third panel pair ($\lambda = 2L_z$), waves radiated by the third panel pair cancel each other in the normal direction of the panel pair in space. Because of the comparatively large vibration amplitude of the panel pair (the amplitude is about $\frac{2}{3}$ of the amplitude of the dominant pair), the wave interference leads to a large decreasing slope of the radiation efficiency curve. When $\gamma = 0.37$ where the acoustic wavelength λ equals twice the distance of the dominant panel pair ($\lambda = 2L_x$), waves radiated by the dominant panel pair also cancel each other in the normal direction of the pair in space. As a result, the slope of the modal radiation efficiency changes from positive to either zero or negative. The plateau continues until $\gamma > 0.48 (\lambda < 4/3L_z)$ where the destructive wave interference in the normal direction of the third panel pair ends. After this γ, the slope becomes positive again due to the increasing constructive interference of waves radiated by the third panel pair and the decreasing destructive interference of waves radiated by the dominant panel pair. The wave cancellation of the dominant panel pair stops at $\gamma = 0.55 (\lambda = 4/3L_x)$. Above this γ, the radiation efficiency curve is dominated by the edge radiation leading to a near constant slope before the critical frequency.

Sound radiation of mode $[D\_AS(4,1), AS(4,1)^*, S(2,4)^*]_{93.0\,\mathrm{Hz}}$ is dominated by the vibration of the two asymmetrical panel pairs due to the much smaller vibration amplitude of the symmetrical panel pair. The two-dimensional cross section

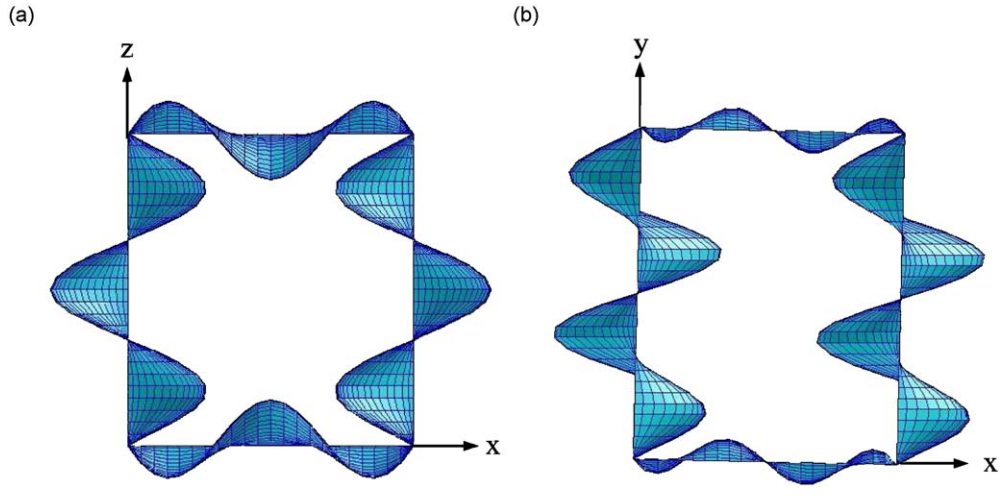

Fig. 4. 2D cross section view of the mode shapes for: (a) Mode $[D\text{-}S(1,3), S(1,3)^*, S(3,1)]_{6.6\,\mathrm{Hz}}$ in x–z plane and (b) Mode $[D\_AS(4,1), AS(4,1)^*, S(2,4)^*]_{93.0\,\mathrm{Hz}}$ in x–y plane.

(parallel to the x–y plane) mode shape distribution of the two asymmetrical panel pairs is shown in Fig. 4(b). The effect of wave interference for this mode can be observed after $\gamma > 0.24(\lambda < 2L_y)$ where the modal sound radiation of the box is no longer a single sound source because the acoustic wavelength is less than twice of the largest box dimension. The rate of decreasing slope is small initially due to the comparatively smaller vibration amplitude of the non-dominant asymmetrical panel pair (about $\frac{1}{4}$ of that of the dominant pair). The slope decreases much rapidly after $\gamma = 0.32(\lambda = 2L_x)$ because of the increasing phase difference of sound radiated by the dominant panels. The slope decreases continually but remains positive well pass $\gamma = 0.36(\lambda = 4/3L_y)$ where wave cancellation in the normal direction of the non-dominant asymmetrical pair begins. The slope changes from positive to negative when the wavenumber ratio increases to $\gamma = 0.48(\lambda = 4/3L_x)$ where wave radiated by the non-dominant panel pair cancels each other completely in their normal direction ($\lambda = L_y$). Destructive wave interference in the normal direction of the dominant panel pair also begins after this γ. The plateau continues until $\gamma = 0.64(\lambda = 3/4L_y)$ where wave cancellation in the normal direction of the non-dominant asymmetrical panel pair ends. After this γ, the slope of radiation efficiency is dominated by the edge radiation until the frequency reaches the critical frequency.

Because all panels of this mode have low-high mode number and either (even, odd) or (even, even) mode shape distribution of simply supported panels, the mode has higher radiation efficiency than that of other modes in the group in the low and medium frequency ranges as shown in Fig. 3(e). This observation is similar to the higher radiation efficiency of low-high number (even, odd) or (even, even) modes of simply supported panels when comparing to that of the low–low number modes [2]. Similar features can also be found in the modal radiation characteristics of other groups (Fig. 3(b)–(f)).

3.4. Modal radiation efficiencies in the high frequency range

Radiation efficiencies of the box modes always have a peak at frequencies just above the critical frequency ($\gamma = 1$). This is also the case for single panels as reported in Refs. [2,3]. Above the critical frequency, modal radiation efficiency of a panel can be approximated by [3,13]

$$\sigma_{m,n} \cong \frac{1}{[1-(k_p/k)^2)]^{1/2}} > 1. \tag{5}$$

In the case of single panels, the height of the peak increases with modal indices [13]. However, this is not always the case for the box modes due to the complex three dimensional mode shapes and the interference of sound radiated by the component panels, although the general trend can still be observed. The radiation efficiency σ converges to unity for all box modes at $\gamma \gg 1$, which is the same as that observed for simply support panel modes.

3.5. The effect of volume displacements

It was shown previously that the large volume displacement modes (either globally as monopole or locally as dipole, quadrupole and octopole) always have higher radiation efficiency than the other modes in their own group for small γ. These modes are mode $[S(1,1), D\_S(1,1), S(1,1)]_{23.0\,\mathrm{Hz}}$, mode $[S(2,1), AS(1,1), D\_S(1,2)]_{35.8\,\mathrm{Hz}}$, mode $[D\_S(2,2), AS(1,2), AS(1,2)]_{52.7\,\mathrm{Hz}}$ and mode $[AS(2,2)^*, D\_AS(2,2), AS(2,2)]_{71.0\,\mathrm{Hz}}$ whose vibration mode shape is close to that of an ideal monopole, dipole, quadrupole and octopole, respectively. Radiation efficiency curves of these modes are represented by the thin solid lines without marker in Fig. 3(a)–(d).

It is noticed that mode $[AS(3,1)^*, D\_S(2,1), S(2,1)]_{43.5\,\mathrm{Hz}}$ has much lower radiation efficiency than any other mode in the same group for small values of γ (see Fig. 3(b)). The mechanism leading to this phenomenon can be explained from the vibration distribution of the box mode and the characteristics of modal radiation efficiencies of simple supported panels. In plate panels, the (odd, odd) modes have much higher radiation efficiency than that of (odd, even) modes at low frequencies. The radiation efficiencies of (odd, odd) modes also depend upon the net volume displacements [2]. While for this box mode, the mode shape of the only (odd, odd) panel pair is largely distorted from that of the $(3,1)$ simply supported panel mode and has the smallest amplitude within the three panel pairs. Very little net-volume displacement is generated locally by the (odd, odd) panel pair in addition to the zero net-volume displacement of the mode. Therefore, much less sound is radiated by the vibration of the mode at low γ as compared to the other modes in the group.

3.6. Effects of the mode shape distribution of the dominant panels

The importance of the mode shape distribution of the dominant panel pair to sound radiation characteristics of the box modes is studied by comparing the radiation efficiency of the fundamental mode in each of the six groups as shown in Fig. 5.

Similar to radiation characteristics of simply supported panels, modes whose dominant panels have (odd, odd) mode shapes are more effective sound radiators than others for small γ. Modes having (even, odd) or (odd, even) shape dominant panels are better sound radiators than modes having (even, even) shape dominant panels. The only exception is the large (global or local) volume displacement modes discussed in Section 3.5, which can have higher radiation efficiency than modes not in their own category at low γ. One example is mode $[D_S(2,2), AS(1,2), AS(1,2)]_{52.7\,\mathrm{Hz}}$which generates a large

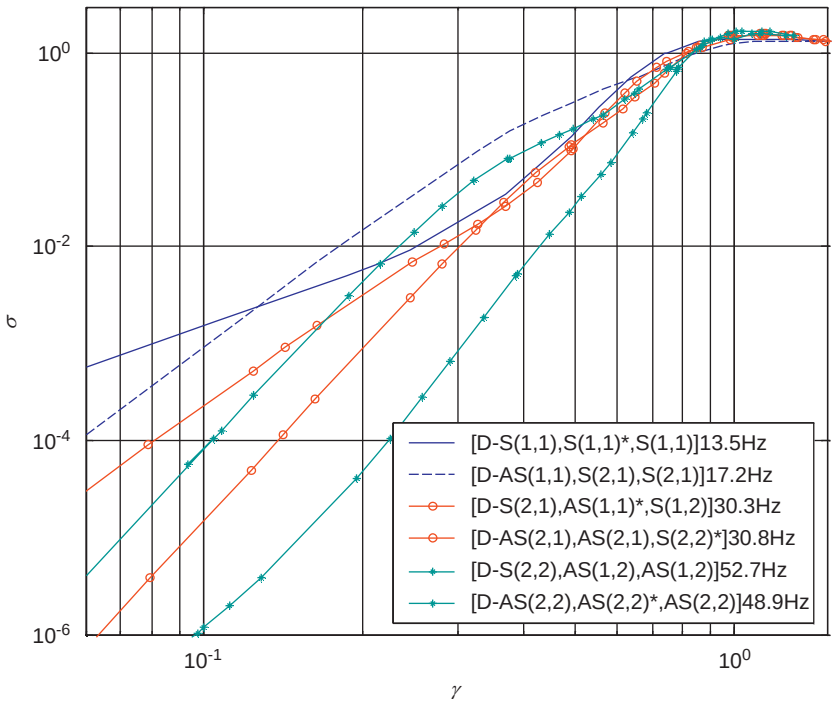

Fig. 5. Comparison between the modal radiation efficiencies of the fundamental modes in the six groups.

local volume displacement at each quarter of the box corresponding to the (2, 2) shape of the dominant panel pair. Thus, the mode can have higher radiation efficiency than modes having (odd, even) or (even, odd) shape dominant panels at low γ.

3.7. Effects of the relative phase of the dominant panels and the adjacent panels

The relative phase of the dominant panels and the adjacent panels also plays an important part in determining the sound radiation of the box modes. Effects of the relative phase of the dominant panels on sound radiation characteristics of the box modes are studied in this paper by comparing the radiation efficiency of mode $[D\_S(1,1),S(1,1)^*,S(1,1)]_{13.5\,\mathrm{Hz}}$ and mode $[D\_AS(1,1),S(2,1),S(2,1)]_{17.2\,\mathrm{Hz}}$. Both modes have the same dominant panel pair, and have the same (1, 1) mode shape installed in the dominant panels. However, because the dominant panel pair of the former is symmetrical and the latter is asymmetrical, the two modes have very different radiation patterns. The former behaves as a monopole and the latter as a dipole for low γ so that the former has higher radiation efficiency than the latter mode at low γ. However, because the vibration of the two non-dominant panel pairs of mode $[D\_S(1,1),S(1,1)^*,S(1,1)]_{13.5\,\mathrm{Hz}}$ is out of phase to the dominant panel pair, a small net-volume displacement is generated [1]. This results in a much weaker monopole than an ideal one. On the other hand, most of the vibration energy of mode $[D\_AS(1,1),S(2,1),S(2,1)]_{17.2\,\mathrm{Hz}}$ is installed in the dominant panel pair, a relatively stronger dipole is formed (see Fig. 3(f)). A dipole has a 40 dB/decade increase in radiation efficiency while a monopole only has a 20 dB/decade increase in radiation efficiency, the small different in radiation efficiency of the two modes at low γ is quickly overcome by the faster increase radiation efficiency of mode $[D\_AS(1,1),S(2,1),S(2,1)]_{17.2\,\mathrm{Hz}}$. Thus, the mode becomes a much effective sound radiator than mode $[D\_S(1,1),S(1,1)^*,S(1,1)]_{13.5\,\mathrm{Hz}}$ in the medium frequency range.

Similarly, mode $[D\_S(2,1),AS(1,1)^*,S(1,2)]_{30.3\,\mathrm{Hz}}$ has higher radiation efficiency than mode $[D\_AS(2,1),AS(2,1),S(2,2)^*]_{30.8\,\mathrm{Hz}}$ in both low and medium frequency ranges because the former is close to a dipole sound source and the latter is close to a quadrupole source. For the last pair of modes in Fig. 5, mode $[D\_S(2,2),AS(1,2),AS(1,2)]_{52.7\,\mathrm{Hz}}$ has much higher radiation efficiency than mode $[D\_AS(2,2),AS(2,2)^*,AS(2,2)]_{48.9\,\mathrm{Hz}}$ in the entire low and medium frequency ranges because the former is a strong quadrupole while the latter is a weak octopole.

3.8. Radiation efficiencies of typical box modes and the corresponding simply supported panel modes

In the previous sections, we found that the mode shape and phase distribution of the box panels determines the radiation characteristics of the structure. In this section, the relationship between modal radiation efficiencies of the box

modes and those of the corresponding simply supported panel modes are studied because mode shapes of simply supported panels are used to describe the vibration distribution of the box modes in this investigation.

A simply supported panel having the same dimensions (surface area $1.15 \times 1\,m^2$ and 2.5 mm in thickness) and same material properties of the largest panel(s) of the box is used in this simulation. The modal radiation efficiencies of three fundamental panel modes, namely: (1, 1), (2, 1) and (2, 2) modes and their corresponding box modes are shown in Fig. 6(a)–(c). It is found that box modes are generally poorer sound radiators than the corresponding simply supported panel modes at low γ except the large volume displacement (either globally or locally) box modes discussed previously (see Fig. 6(a)–(c)). This is due to wave interference between sound radiated by the component panels of the box.

On the contrary, the radiation efficiency of the large volume displacement box modes is higher than that of the corresponding single panel mode for $\gamma < 1$. This can be explained by the three dimensional nature of the box modal vibration. Sound radiation of the large volume displacement box modes resembles the three-dimensional (3D) elementary sound sources, i.e., 3D monopole, dipole, quadrupole or octopole. On the other hand, sound radiation of simply supported panel modes can be represented by that of the two dimensional (2D) sources (2D monopole, dipole, etc.). By comparing sound radiation of a 3D sound source such as a vibrating spherical source to that of a 2D source such as a circular baffled piston, the higher radiation efficiency of a large volume displacement box mode (e.g., mode $[S(1,1), D\_S(1,1), S(1,1)]_{23.0\,Hz}$) than that of a corresponding simply supported panel mode (e.g., the (1, 1) mode) can be understood.

A spherical sound source is a zero-order non-directional sound source, which radiates sound equally in all directions. The radiated sound power of a spherical sound source is given by [15]

$$W_{\text{Sphere}} = 2\pi a^2 v_S^2 \rho_0 c \frac{(ka)^2}{1+(ka)^2}, \tag{6}$$

where a, v_S^2 are the radius and the squared of average surface velocity of the spherical sound source.

On the other hand, sound radiated by a baffled piston is directional. The radiated sound power from a circular baffled piston is given by [11]

$$W_{\text{Piston}} = \tfrac{1}{2} v_P^2 [C_v + \rho_0 c \pi a^2 R(2ka)], \tag{7}$$

where C_v represents the mechanical damping term of the baffled panel, v_P is the average surface velocity of the piston and $R(2ka)$ is the resistive function which is given by [11]

$$R(2ka) \approx \frac{(ka)^2}{2}, \quad 2ka \ll 1. \tag{8}$$

If we neglect the mechanical damping term in Eq. (7), the radiated sound power of the baffled piston at low frequencies becomes

$$W_{\text{Piston}} \approx \frac{1}{2}\pi a^2 \rho_0 c v_P^2 \left[\frac{(ka)^2}{2}\right]. \tag{9}$$

The non-dimensional radiation efficiency of the two sound sources can now be obtained from the radiated sound power of the sources as

$$\sigma_S = \frac{W_{\text{Sphere}}}{4\pi a^2 \rho_0 c v_S^2} = \frac{(ka)^2}{2[1+(ka)^2]}, \tag{10a}$$

and

$$\sigma_P = \frac{W_{\text{Piston}}}{\pi a^2 \rho_0 c v_p^2} \approx \frac{(ka)^2}{4}, \quad ka \ll 1, \tag{10b}$$

where σ_S and σ_P is the radiation efficiency of the spherical and the circular baffled piston sound sources, respectively.

Comparing Eq. (10a) with Eq. (10b) we found that a spherical sound source has much higher radiation efficiency than a baffled piston for $\gamma \ll 1$. The higher radiation efficiency of other large volume displacement modes of the box as compared to the corresponding simply supported panel modes can also be explained in similar manners.

4. Modal radiation directivities

This section examines the successively change of sound radiation directivity patterns of the box modes. The radiation patterns of the large volume displacement modes of the box are of particular concern because of their high modal sound radiation efficiencies. Effects of the rigid body box oscillation due to flexural vibration of asymmetrical panel pair(s) of a box mode [1] on modal sound radiation of the box are examined for a typical mode from each of group (D_AS, AS, S) and group (D_AS, S, S).

The edge (or strip) and surface radiation patterns of simply supported panels have been well discussed in many literatures (i.e., Refs. [3,4,11]). Similar radiation patterns can also be observed for the box modes although the control

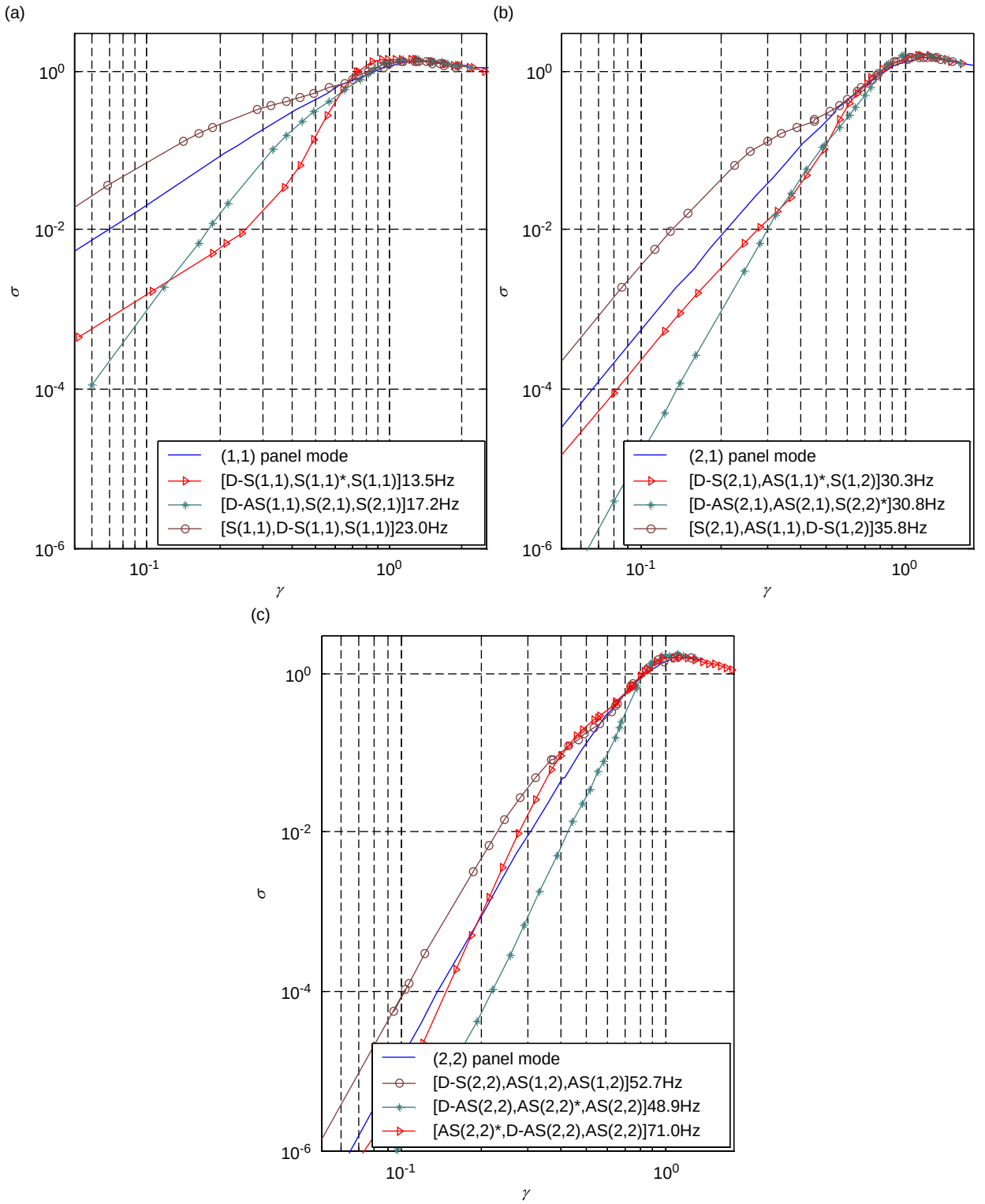

Fig. 6. Radiation efficiencies of the fundamental simply supported panel modes and the corresponding modes of the box-type structure: (a) (1,1) mode; (b) (2,1) mode; and (c) (2,2) mode.

mechanism may not be identical. In this paper, the term "edge radiation pattern" is defined as where the sound pressure distribution in space corresponding to the box edges is higher than that of other locations. The term "surface radiation pattern" is defined as where the sound pressure distribution in front of the panels is closely represented by the vibration mode shape and amplitude distribution of the box panels.

4.1. Radiation directivities of the large volume displacement modes

Fig. 7 shows the evolution of radiation directivities of mode $[S(1,1), D\_S(1,1), S(1,1)]_{23.0\,\mathrm{Hz}}$ at frequencies below and above the critical frequency. For this box mode, all the plate panels vibrate in phase producing a large net-volume displacement (see Ref. [1, Fig. 4] for visualization of the mode). The net-volume displacement controls the sound radiation of the mode at low γ ($\gamma<0.2$) where the acoustic wavelength is much larger than the largest box dimension. The modal radiation directivity resembles a monopole radiation pattern in this frequency range (see Fig. 7(a) and (b)). However, because of the uneven vibration amplitude distribution in the three panel pairs, the radiation directivity differs lightly from that of a perfect spherical monopole. The distortion in the sound field increases as γ increases due to the increasing sound pressure difference radiated by the three panel pairs as a result of increasing modal sound radiation efficiency. As γ increases to where the acoustic wavelength becomes smaller than twice the largest box dimension ($\gamma>0.57$), the strengthening wave interference leads to a smaller pressure distribution in the normal direction of each panel pair (see Fig. 7(c) and (d)).

As the frequency increase further ($0.7<\gamma<1$), the pressure distribution in space corresponding to the box corners is higher than that of the box edges, while pressure distribution corresponding to the edges are higher than that of the panel surfaces. This can be explained by the box-type configuration of the structure such that sound pressure in space corresponding to a box edge is the in-phase superposition of sound pressure radiated by the two adjacent panels forming the edge, and sound pressure corresponding to a box corner is the superposition of the three adjacent panels forming the corner. The pressure difference is insignificant at low γ since sound radiation of the mode is net volume displacement control. However, the pressure difference increases as γ increases and becomes prominence at higher γ. Consequently, the modal sound radiation is dominated by the edge radiation pattern in the medium frequency range as shown in Fig. 7(c) and (d). As γ increases above the unity, the edge radiation pattern diminishes and evolves to a surface radiation where six lobes perpendicular to the six panels emerges and characterizes the sound field pressure distribution (see Fig. 7(e) and (f)). In this γ range, sound pressure distribution in front of each panel takes the form of the vibration mode shape and amplitude distribution of the panel. Other modes in group (D_S, S, S) also form monopole sound source in the low frequency range.

For mode $[S(2,1), AS(1,1), D\_S(1,2)]_{35.8\,\mathrm{Hz}}$ (see Ref. [1, Fig. 6]), the six panels of the box vibrate such that the plane at $y=L_y/2$ divides the box into two halves vibrating asymmetrically. The radiation directivity of this mode resembles a dipole source for $\gamma<0.42$ (see Fig. 8(a) and (b)). However, when the acoustic wavelength becomes smaller than twice the plate edges of the dominant panels ($\gamma>0.42$), edge radiation pattern emerges and affects the sound field pressure distribution. As γ increases further, the edge radiation pattern becomes prominence and dominates the sound field pressure distribution (see Fig. 8(c)–(e)). Concurrently, the pressure distribution in the normal direction of the asymmetrical panel pair reduces to a minimum due to both diminishing effect of volume displacement and wave interference of the asymmetrical panel pair, which begins at $\gamma=0.63(\lambda=4/3L_y)$. As γ increases and passes the unity, the edge radiation pattern diminishes and is replaced by the surface radiation pattern. The pressure distribution in space closely corresponds to the vibration amplitudes and mode shapes of the component panels (see Fig. 8(f)). The asymmetry of the box mode with respect to the plane at $y=L_y/2$ leads to the minimum pressure distribution on the $y=L_y/2$ plane for all values of γ. Other modes in group (D_S, S, AS), modes in group (D_AS, S, S) also form dipole sound sources at low frequencies.

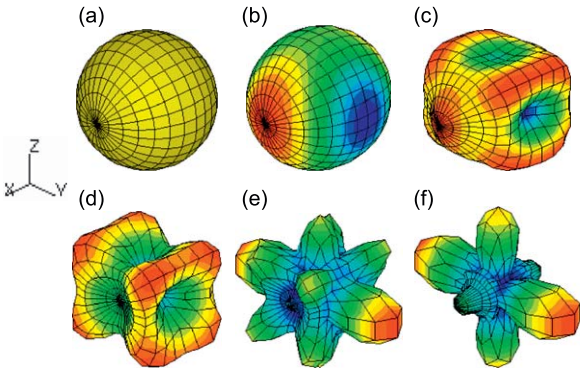

Fig. 7. Radiation directivities of mode $[S(1,1), D\_S(1,1), S(1,1)]_{23.0\,\mathrm{Hz}}$ at: (a) $\gamma=0.07$; (b) $\gamma=0.19$; (c) $\gamma=0.75$; (d) $\gamma=0.94$; (e) $\gamma=1.50$; and (f) $\gamma=1.80$.

For mode $[D\_S(2,2), AS(1,2), AS(1,2)]_{52.7\,\mathrm{Hz}}$ (see Ref. [1, Fig. 8]), the two planes at $y = L_y/2$ and $z = L_z/2$ divide the box into four parts. Elements in each part vibrate in phase, and are out of phase with elements of the adjacent parts. Therefore, the mode has a quadrupole sound radiation pattern at low γ (see Fig. 9(a)–(c)). Other modes in group (D_S, AS, AS), modes in group (D_AS, AS, S) also form quadrupole sound sources in the low frequency range.

The vibration distribution of mode $[AS(2,2)^*, D\_AS(2,2), AS(2,2)]_{71.0\,\mathrm{Hz}}$ (see in Ref. [1, Fig. 9]) divides the box into eight equal parts. Such vibration pattern leads to an octopole sound radiation pattern at $\gamma < 1$. The eight lobes of the octopole emerge from the eight corners of the box (see Fig. 10(a)–(d)). After the critical frequency ($\gamma > 1$), the original octopole

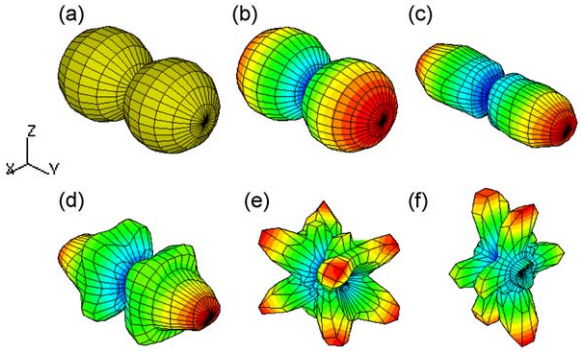

Fig. 8. Radiation directivities of mode $[S(2,1), AS(1,1), D\_S(1,2)]_{35.8\,\mathrm{Hz}}$ at: (a) $\gamma = 0.09$; (b) $\gamma = 0.15$; (c) $\gamma = 0.60$; (d) $\gamma = 0.75$; (e) $\gamma = 1.21$; and (f) $\gamma = 1.80$.

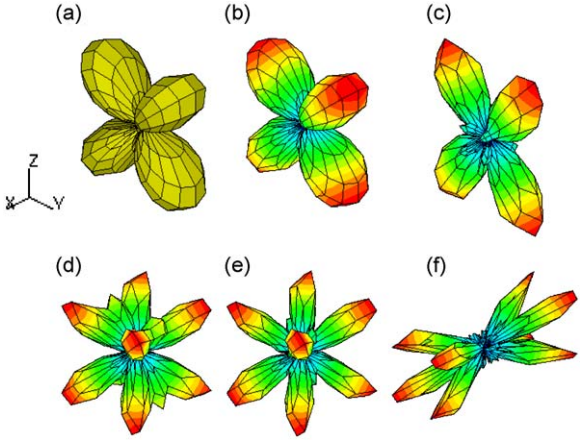

Fig. 9. Radiation directivities of mode $[D\_S(2,2), AS(1,2), AS(1,2)]_{52.7\,\mathrm{Hz}}$ at (a) $\gamma = 0.10$; (b) $\gamma = 0.12$; (c) $\gamma = 0.62$; (d) $\gamma = 0.94$; (e) $\gamma = 1.00$; and (f) $\gamma = 1.80$.

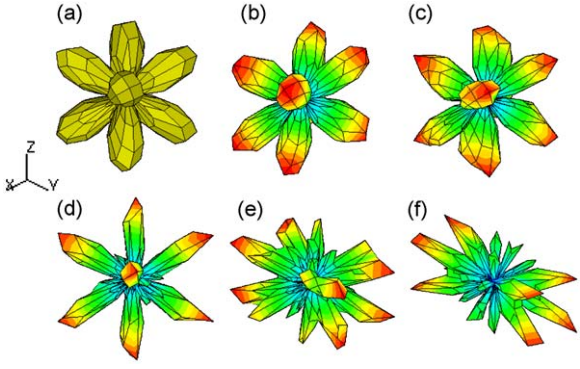

Fig. 10. Radiation directivities of mode $[AS(2,2)^*, D\_AS(2,2), AS(2,2)]_{71.0\,\mathrm{Hz}}$ at: (a) $\gamma = 0.12$; (b) $\gamma = 0.54$; (c) $\gamma = 0.86$; (d) $\gamma = 1.07$; (e) $\gamma = 1.50$; and (f) $\gamma = 1.80$.

radiation pattern evolves into a complicated surface radiation pattern, where the sound field in front of each panel correlates to the vibration amplitude and mode shape of the corresponding panel (Fig. 10(e)–(f)). Other modes in the same group also form octopole sound sources in the low frequency range.

4.2. Effects of rigid body oscillations on sound radiation of box modes

In Ref. [1], we identified two types of rigid body oscillations in the box modal vibration due to the flexural motion of asymmetrical panels, namely, the whole body piston-like oscillation and the whole body rotation oscillation. The mechanism leading to the rigid body oscillations has been explained [1]. The effect of the rigid body oscillation on the sound radiation of the box modes is studied in this section. Two typical modes are chosen for this study, one from group (D_AS, AS, S), the other is from group (D_AS, S, S).

The mode shape distribution of mode $[D\_AS(2,1), AS(2,1), S(2,2)^*]_{30.8\,\mathrm{Hz}}$ is shown in Fig. 2. Vibration of the mode consists of two components: one is the flexural vibration of the box panels; the other is the whole body rotational oscillation about an axis connecting the geometry center of the pair of the symmetrical panels. These two components are superimposed on each other such that the two quadrupoles produced by them are in opposite phase as shown in Fig. 11(a). However, because the vibration power of the rotational oscillation is <2 percent of the input power of the flexural vibration of the mode, the overall acoustic field is dominated by the sound pressure radiated by the flexural vibration of the panels even though both vibration motions have similar values of radiation efficiency as indicated in Fig. 11(b)–(d).

Vibration of mode $[D\_AS(1,1), S(2,1), S(2,1)]_{17.2\,\mathrm{Hz}}$ also consists of two components: one is the flexural vibration of the box panels; the other is the whole body piston-like oscillation in the normal direction of the asymmetrical panel pair. The two components are such that the dipole produced by one of them is in opposite phase to the dipole produced by the other as illustrated in Fig. 12(a). Contributions of the whole body piston-like oscillation and the flexural vibration of the box panels to the sound field are demonstrated in Fig. 12(b)–(d). Similar to that of the previous case, the vibration power of the piston-like oscillation is much less than that of the flexural vibration of the panel, the overall acoustic field is therefore dominated by the sound pressure radiated by the flexural vibration. The radiation efficiency of the box mode is smaller than that due to the flexural vibration along as a result of the out of phase interference between sounds radiated by the two vibration components.

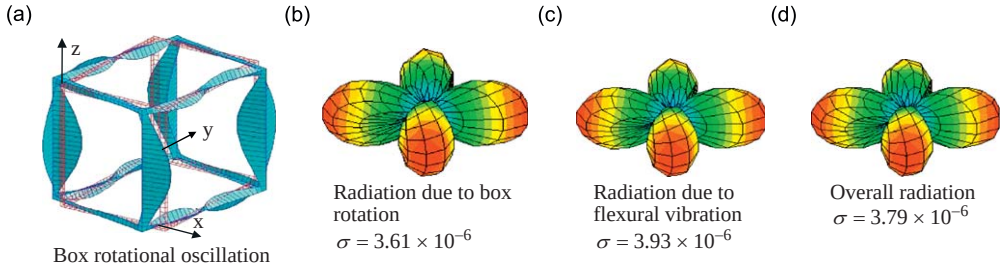

Fig. 11. Rigid body rotational oscillation of mode $[D\_AS(2,1), AS(2,1), S(2,2)^*]_{30.8\,\mathrm{Hz}}$ and its effect to the sound radiation pattern of the mode at 30.8 Hz: (a) isometric view; (b) sound radiation pattern due to the box rotational oscillation only; (c) sound radiation pattern due to flexural vibration only; and (d) sound radiation pattern due to the combined vibration motions.

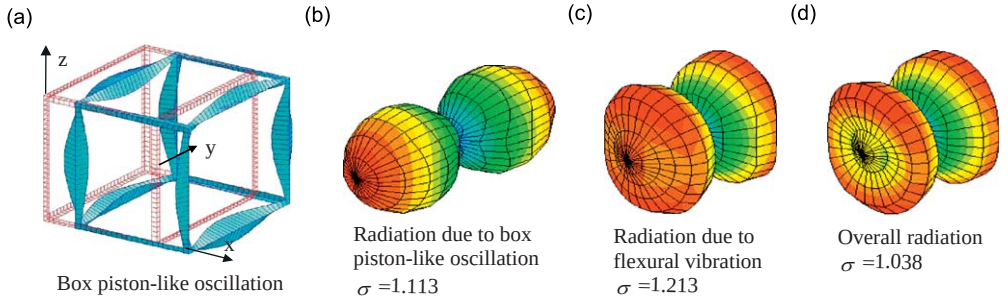

Fig. 12. Rigid body piston-like oscillation of mode $[D\_AS(1,1), S(2,1), S(2,1)]_{17.2\,\mathrm{Hz}}$ and its effect to sound radiation pattern of the mode at 250 Hz: (a) Isometric view; (b) sound radiation pattern due to box piston-like oscillation only; (c) sound radiation pattern due to flexural vibration only; and (d) sound radiation pattern due to the combined vibration motions.

5. Discussion and concluding remarks

The finite element and boundary element methods are used to study the characteristics of sound radiation from a box-type structure. This study shows that the classification of vibration modes of a box structure into six groups is also meaningful for the study of modal sound radiation of the complex vibration modes of the box structure.

The general features of modal sound radiation in each group are disclosed and explained by the mode shape, symmetry properties and the phase relationship between the component panels of a box mode. Characteristics of modal sound radiation efficiency at different frequency ranges are discussed. It is found that in the low frequency range where the wavenumber ratio is small, modal radiation efficiencies of the box modes are controlled by volume displacements of the box vibration. The slope of modal radiation efficiency curves is similar to that of a simply supported panel mode having the same modal indices of the dominant panels of the box mode in this frequency range. In the medium frequency range where the acoustic wavelength is smaller than twice the box dimension but greater than the structural wavelength, plateau or change in slope is observed in the radiation efficiency curves of higher order box modes resulting by the interference of sound radiated by the component panels of the box. Volume displacement, mode shape distribution and the relative phase between panels control the radiation efficiency and sound pressure distribution of the box modes in the low and medium frequency ranges. Similar to that of simply supported panel modes, the radiation efficiency of all box modes reaches a peak above the critical frequency, and gradually converges to unity at $\gamma \gg 1$. Although higher order modes (other than the (odd, odd) modes) of a simply supported panel always have higher radiation peaks, it is not always the case for the radiation efficiency of the box modes due to the interference of sound radiated by the box panels.

The change of radiation directivity patterns for the large volume displacement modes as a function of the wavenumber ratio is observed in this study. Simple sound radiation patterns (namely, monopole, dipole, quadrupole and octopole patterns) are identified in the six groups of modes at low frequencies ($\gamma \ll 1$). In the medium frequency range, edge radiation patterns become obvious, where lobes of high sound pressure levels emerge from the edges of the box. The edge radiation pattern becomes surface radiation patterns at frequencies greater than the critical frequencies, where mode shape and amplitude distribution of the box panels characterizes the radiation pattern and pressure distribution in the sound field.

In this work, common features of modal sound radiation of a box type structure are disclosed to provide an understanding to effectively control the noise radiation of such structures for industry applications. Although the results of only one box structure are used in the study, the vibration and sound radiation characteristics unveiled in this work and in Ref. [1] are also meaningful for box structures of other dimensions. Increasing complexity of vibration and sound radiation analysis arising from a practical box structure with reduced symmetry can also be analyzed using similar approach outlined in this work and in Ref. [1]. The information of modal vibration and sound radiation characteristics of a box structure provided by Ref. [1] and this paper can also be utilized to predict the vibration response and noise radiation of a box structure under external excitations.

The effects of boundary conditions and geometrical perturbations of box type structures to the boundary coupling mechanism, vibration and sound radiation of an idealized box-type structure were studied previously by the first author [14]. The boundary coupling mechanism of a box-type structure has also been discussed briefly in Ref. [1]. It was found that the boundary energy flow for modes in groups (D_S, S, S) and (D_AS, AS, AS) is dominated by bending moment. The boundary conditions for mode in these two groups are mostly close to the simply supported conditions. Thus the modal vibration and sound radiation characteristics for these two mode groups are not affected by imposing simply supported boundary conditions to the box edges. For modes in the other groups, the boundary energy flow are governed by both shear force and bending moment. The vibration amplitude distribution in some panel pairs would be affected (slightly) if simply supported boundary conditions are imposed to their coupling boundaries due to the exclusion of the part of energy flow by the shear force coupling. However, the effect to the mode shape distribution of the box is negligible since the mode shape distribution in the panels is controlled by the wave matching condition between the plate bending wave and the physical dimension of the box panels. As a result, the overall effect of simply supported boundary conditions (imposed to all or some box edges) to the modal vibration of a box type structure is insignificant.

The detailed change at the box boundaries has little effect to the modal radiation efficiency and radiation directivity of the box modes at low frequencies. At low frequencies, the sound radiation is determined by the overall magnitude and local volume displacements. As a result, the radiation properties of the box structure can be reasonably described by simple monopole, dipole and quadrupole sound sources as illustrated in Figs. 7–10.

Due to the changing modal amplitude distribution when boundary conditions are imposed to the box edges, the modal radiation efficiency for modes in groups other than (D_S, S, S) and (D_AS, AS, AS) are affected by such changes although the general trend of modal radiation efficiency for each group remains unchanged as those presented in Fig. 3. Wavenumber analysis of sound radiation from baffled plate has shown that the near-field flexural vibration could affect the wavenumber spectrum of the modal vibration, thus the far-field radiation of the acoustically slow sound [13].

Acknowledgment

Useful discussion with, and advice from Dr. Nabil H. Farag for this work is gratefully appreciated by the authors.

References

[1] T.R. Lin, J. Pan, Vibration characteristics of a box-type structure, *Journal of Vibration and Acoustics, Transactions of ASME* 131 (2009) 031004-1–031004-9.
[2] C.E. Wallace, Radiation resistance of a rectangular panel, *Journal of the Acoustical Society of America* 51 (1972) 946–952.
[3] G. Maidanik, Response of ribbed panels to reverberant acoustic fields, *Journal of the Acoustical Society of America* 34 (1962) 809–826.
[4] F. Fahy, *Sound and Structural Vibration—Radiation Transmission and Response*, Academic Press, New York, 1985.
[5] C. Wang, J.C.S. Lai, The sound radiation efficiency of finite length acoustically thick circular cylindrical shells under mechanical excitation I: theoretical analysis, *Journal of Sound and Vibration* 232 (2000) 431–447.
[6] H.A. Schenck, Improved integral formulation for acoustic radiation problems, *Journal of the Acoustical Society of America* 44 (1968) 41–58.
[7] A.F. Seybert, B. Soenarko, F.J. Rizzo, D.J. Shippy, An advanced computation method for radiation and scattering of acoustic waves in three dimensions, *Journal of the Acoustical Society of America* 77 (1985) 362–368.
[8] O. von Estorff (Ed.), *Boundary Element in Acoustics: Advances and Applications*, WIT, Southampton, 2000.
[9] A.F. Seybert, X.F. Wu, F.B. Oswald, Validation of finite element and boundary element methods for predicting structural vibration and radiated noise, *Proceedings of Winter Annual Meeting*, ASME, 1992, pp. 1–7.
[10] SYSNOISE Rev 5.3 User's Manual, LMS Numerical Technologies.
[11] M.P. Norton, *Fundamentals of Noise and Vibration Analysis for Engineers*, Cambridge University Press, New York, 1999.
[12] J. Pan, D.A. Bies, The effect of fluid-structural coupling on sound waves in an enclosure—theoretical part, *Journal of the Acoustical Society of America* 87 (1990) 691–707.
[13] M.P. Norton, J. Pan, Noise radiated by baffled plates, in: S. Braun, et al. (Eds.), *Encyclopedia of Vibration*, Academic Press, New York, 2002.
[14] T.R. Lin, Sound and Vibration Characteristics of Box-type Structures, Master's Dissertation, University of Western Australia, New York, 2001.
[15] L. Cremer, M. Heckle, E.E. Ungar, *Structure-borne Sound: Structural Vibration and Sound Radiation at Audio Frequencies*, second ed., Springer, New York, 1988.